Analysis of two choir outbreaks in Germany in 2020 characterizes long- range transmission risks through SARS-CoV-2

Authors: Felix Reichert*# (1,2,3), Oliver Stier# (4), Anne Hartmann# (5) , Claudia Ruscher (6), Annika Brinkmann (1), Marica Grossegesse (1), Markus Neumann (1), Dirk Werber (6), Marius Hausner (7), Mareike Kunze (7), Bettina Weiß (8), Janine Michel (1), Andreas Nitsche (1), Martin Kriegel (5), Victor M. Corman (9), Terry C. Jones (9,10), Christian Drosten (9), Tobias Brommann (11), Udo Buchholz (1).

*corresponding author: Felix Reichert (**Email:** reichertf@rki.de)

#contributed equally

Affiliations:

(1) Robert Koch Institute, Berlin, Germany

(2) Postgraduate Training for Applied Epidemiology (PAE), Robert Koch Institute, Berlin, Germany

(3) European Programme for Intervention Epidemiology Training (EPIET), European Centre for Disease Prevention and Control (ECDC), Stockholm, Sweden

(4) Siemens AG, Technology, 13623 Berlin, Germany

(5) Technical University of Berlin, Hermann Rietschel-Institute, Berlin, Germany

(6) State Office for Health and Social Affairs, Berlin, Germany

(7) Local health authority “Berlin-Mitte”, Berlin, Germany

(8) Local health authority “Charlottenburg-Wilmersdorf”, Berlin, Germany

(9) Institute of Virology, Charité-Universitätsmedizin Berlin and German Centre for Infection Research (DZIF), Associated Partner Site at Charité - Universitätsmedizin Berlin, Charitéplatz 1, 10117, Berlin, Germany.

(10) Centre for Pathogen Evolution, Department of Zoology, University of Cambridge, Downing St., Cambridge, CB2 3EJ, U.K.

(11) Berlin Cathedral Choir, Berlin, Germany

Competing Interest Statement:

Oliver Stier is named as inventor on a patent application filed recently regarding the determination of potentially infectious aerosol air concentrations.

Victor M. Corman is named on a patent application filed recently regarding the diagnostic of SARS-CoV-2 by antibody testing.

Terry C. Jones is in part funded through NIAID-NIH CEIRS contract HHSN272201400008C.

Key words:

SARS-CoV-2, Singing, Disease Outbreaks, Aerosols, Dose-Response Model

Abstract

Background: Superspreading events are important drivers of the SARS-CoV-2 pandemic. By analyzing two outbreaks associated with choir rehearsals in March 2020, we demonstrate the risk of indoor, long-range (LR) transmission and singing, to help prevent similar outbreaks.

Methods: We conducted two retrospective cohort studies and obtained demographic, clinical, laboratory and contact data, performed SARS-CoV-2 serology, whole genome sequencing (WGS), calculated LR transmission probabilities, measured particle emissions of selected choir members, and calculated particle air concentrations and inhalation doses.

Results: We included 65 (84%) and 42 (100%) members of choirs 1 and 2, respectively. WGS confirmed strain identity in both choirs and the primary case of choir 1 (transmitting presymptomatically). Particle emission rate when singing was 7 times higher compared to talking. In choir 1, the median concentration of primary cases' emitted particles was 8 times higher, exposure at least 30 minutes longer and room volume smaller than in choir 2, resulting in markedly different estimated probabilities for LR transmission (median: 89% vs. 18%, 95%CI: 80-95% vs. 6-36%). Observed AR in choir 1 (89%) was significantly higher than in choir 2 (24%). According to a risk model, first transmission in choir 1 occurred likely after 7 minutes of singing. The number of inhaled particles emitted by an infectious case, sufficient to infect 50% of exposed, was calculated to 1039-2883 particles (95%CI).

Conclusions: Even in large rooms, singing of an infectious person may lead to secondary infections through LR exposure within minutes. Given the potential for presymptomatic infectiousness, greatest caution is required wherever aerosols can accumulate.

Significance statement

Well-investigated examples of long-range transmission via aerosols and its determinants are rare. We compare two SARS-CoV-2 outbreaks related to choir rehearsals and estimate the probabilities of long-range transmission (>1.5m) by identifying the primary cases and assessing contacts and case status. We estimate the particle concentration in the rehearsal rooms based on emission measurements of the primary cases and room characteristics. Secondary infection rates as high as 90% can occur in several meters distance from the spreader when aerosols cumulate in the breathing air. We present a physical model to interpret our observations and discuss the influencing factors for indoor, long-range transmission. For the virus strain having caused the outbreaks we estimate the dose-response relation of inhaled infectious aerosol.

Introduction

Cluster and superspreading events are believed to have a larger impact on the dynamic of the pandemic than many single cases with few or no onward transmission [1]. Choir rehearsals have been associated with high attack rates [2, 3]. However, previous analyses of outbreaks had to make strong assumptions (such as the number of infectious cases), lacked measurements (such as the particle emission of individuals) or did not tease apart the separate contribution of short-range (SR) vs. long-range (LR) transmission [2-4].

While the respiratory route is considered the main transmission route of SARS-CoV-2 it can be coarsely divided into SR transmission (within 1.5 meter of the source case) and LR transmission (any location in the room). Since the vast majority of emitted particles of an infectious person during breathing, speaking, singing, and even coughing are small enough to be able to float in the air [5], and since amplifiable SARS-CoV-2 virus has been identified in aerosolized particles [6], it is thought that SR transmission is mediated by aerosol or (ballistic) droplets, whereas LR transmission is mediated by aerosols only.

LR (aerosol) transmission occurs probably exclusively indoors and depends on several factors, such as the number of infectors, the particle emission rate and duration, the space volume and ventilation efficiency of the premises where exposure is taking place, as well as the exposed persons' pulmonary ventilation rate and period of particle inhalation [7, 8].

In the beginning of March 2020, the first COVID-19 wave was hitting Berlin. While the first case of COVID-19 was reported in Berlin on 02 March 2020, retrospective analyses showed that, at that time, the COVID-19 epidemic was already in upward swing with a peak in infections around 15 March 2020. On Monday, 09 March 2020, the choir of the Berlin cathedral (choir 1) gathered for the weekly rehearsal. The choir director led a rehearsal of another choir (choir 2) on Thursday, 12 March 2020. On Saturday, 14 March 2020, a member of choir 1 informed the choir director of a positive test for SARS-CoV-2. The choir director informed the local health authority (LHA) about the case and the recent rehearsal. Promptly, choir members were put on 14-day quarantine, however, it turned out that many of them already had developed symptoms. Beginning on Sunday, 15 March 2020, also members of choir 2 started to feel ill.

We investigated the outbreaks with the following objectives:

- To describe the outbreaks
- To identify the source case(s)
- To examine the role of singing and speaking
- To assess the contribution of short and long-range transmission

With the analysis of the two outbreaks, we aim to provide information for the prevention of similar outbreaks in the future.

Methods

Epidemiological outbreak investigation

Study population

We considered the study population in choir 1 as all persons attending any of the last 3 rehearsals,

i.e., on 09 March, 07 March, and 02 March 2020 since several transmission events might have been possible. In choir 2 the study population consisted of all persons attending the rehearsal on 12 March 2020.

Data collection

We conducted exploratory interviews with the choir director and key persons from the choirs. We distributed a paper-based questionnaire to the study population of choir 1 in May 2020. Questions to choir 1 included illness before the rehearsal on 09 March 2020, known possible exposure by other COVID-19 cases, travel, illness (and clinical symptoms) within two weeks before or after the rehearsal, close distance exposure to other choir members during conversations in the context of the rehearsal, seating during the rehearsal and laboratory confirmation by PCR or serology. Answers were entered pseudonymized into a database using epidata (version 2.0; https://www.epidata.dk). Data were checked for entry errors, and plausibility checks were performed before analysis.

In choir 2, structured phone interviews were conducted by one of the authors (OS), a board member of the church congregation in September 2020. Questions to choir 2 included illness (and clinical symptoms) within two weeks after the rehearsal on 12 March 2020, possible alternative explanations for the illness, such as travel, exposure to the choir director (distance and duration), seating during the rehearsal and laboratory confirmation by PCR or serology.

Identifying date of transmission and primary case (Choir 1)

To identify the date(s) of transmission in choir 1, risk ratios (RR) and population attributable fractions (PAF) (((RR-1)/RR)*proportion of cases exposed) were calculated for rehearsal dates including all laboratory-confirmed infections among all members of choir 1. To evaluate possible sources of transmission for choir 1, we explored all choir members who indicated an illness potentially consistent with COVID-19 starting from the 10 days before through two days after the identified transmission date. We assessed exposure, symptoms, laboratory-confirmation, secondary cases, and possible transmission chains.

Cohort study

Cohorts:

For outbreak description and further analyses, we defined the cohorts as potentially susceptible choir members that attended the respective transmission events. Therefore, the primary cases didn´t form part of the cohort.

Additionally, choir members whose infection might have occurred somewhere else were excluded from further analyses. This applied to members of choir 1:

1) with a sequenced strain other than the outbreak strain

2) with serologically confirmed infection who had neither acute symptom onset nor positive SARS-CoV-2 PCR (if done) within two weeks after the rehearsal date.

Case definition choir 1:

We defined a confirmed case as a person who had attended the rehearsal on 09 March 2020, was laboratory confirmed (by either PCR or serology) and had illness onset (with any of the symptoms asked), or had been tested positive by SARS-CoV-2 PCR within two weeks after the rehearsal date.

A possible case had attended the rehearsal on 09 March 2020, had acute onset of at least one respiratory or two general, non-respiratory symptoms within two weeks after the rehearsal date, but

no laboratory test was done.

Case definition choir 2:
The same case definitions applied for choir 1, but referring to the rehearsal on 12 March 2020, instead.

Analysis:
Cases and non-cases are described regarding exposure, age, sex, incubation time, clinical symptoms, laboratory test results and level of care.
Incubation periods and attack rates (AR) of the two choirs were compared by Kruskal-Wallis-Test.

Serological testing

We invited all members of choir 1 for serological testing to measure anti-SARS-CoV-2 antibodies. The outbreak of choir 2 was known 5.5 months after the rehearsal. Therefore, we invited only those members of choir 2 for serological testing, who were symptomatic after the rehearsal and did not yet have a laboratory test. Blood samples were taken 3.5 and 6.5 months after the rehearsals of choir 1 and 2, respectively.

We performed semiquantitative Euroimmun SARS-CoV-2 IgG antibody ELISA with S1 domain substrate (Euroimmun AG, Lübeck, Germany) according to manufacturer's instructions, with the exception that we used heat-inactivated sera (56 °C, 1 h) and the following cutoffs: ratio < 0.4 (negative), 0.4 ≤ ratio ≤ 3 (borderline), ratio > 3 positive. In addition, we used WANTAI SARS-CoV-2 Ab ELISA (Beijing Wantai Biological Pharmacy Enterprise, Beijing, China) for detection of complete antibodies against SARS-CoV-2 according to manufacturer's instructions, with the exception that we applied 50 µl of serum. All samples negative by both ELISA assays, i.e., with an IgG ratio under 0.4, were considered negative. We further characterized the samples with an IgG ratio in the Euroimmun assay over 0.4 with an in-house neutralization test (NT). Details are described in Supplement A.1. Results were considered positive when NT was positive.

For two choir members, we could not obtain sera for testing and results from earlier ELISA tests performed in routine laboratories were considered.

Sequence typing

We performed sequence typing of virus strains collected from all available specimens of cases involved in either choir outbreak as well as from cases who participated in a party, considered as a possible source outbreak of choir 1. We sequenced swab samples with Illumina- (Illumina, San Diego, CA, USA) and MinION (Oxford Nanopore Technologies, Oxford, United Kingdom). Sequencing methods are described in Supplement A.2.

Phylogenetic trees were constructed by aligning the consensus sequences to chosen SARS-CoV-2 genomes sampled before April 2020 and retrieved from GISAID (https://www.gisaid.org), maximum likelihood analysis with MAFFT and visualization with Auspice, as described by the standard protocol for analysis of SARS-CoV-2 genomes provided by Nextstrain (https://www.nextstrain.org).

Measurement of particle emission rates

We measured the particle emission of a sample of 16 participants of choir 1. Besides the presumable primary case, the choir director as well as 14 additional choir singers (3 x soprano, 5 x alto, 3 x tenor,

3 x bass) took part in the measurements. The measurements were performed in a cleanroom, which is equipped with ULPA-filters and an air change rate of more than 300 1/h, whereas the background concentration of particles (P) is 0 P/m³. The subjects wore special, nearly particle-free clean room compatible clothing, consisting of intermediate garments, gowns and head-covers. The subjects were asked to breath, read out a standardized text (the short story "Nordwind und Sonne"), sing two different songs ("Abschied vom Walde", composed by Felix Mendelssohn Bartholdy and a passage from the "Liverpool Oratorio", composed by Paul McCartney) and the tone "La" in three different volumes (piano, mezzoforte, and forte). Each task took between 10 s (singing one tone) and 30 s (other tasks) and was repeated five times. The average of the five repetitions was calculated. Four subjects were asked to perform the same tasks on two different days to investigate the intraindividual variation.

Environmental investigation

For both choir rehearsals we collected room and ventilation data during on-site visits with the choir director and singers. Based on room measurements we calculated the room space volumes and created a room model with STAR-CCM+ (Siemens Product Lifecycle Management Software Inc.). We extracted outside temperature of the respective days (09 March 2020 for choir 1, and 12 March 2020 for choir 2) from the German Meteorological Service [9].

Predicted infection risk for aerosol transmission (PIRA)

Previously, three of the authors (MK, AH, UB) had published a SARS-CoV-2 adapted model by Wells and Riley [8, 10] to evaluate the risk of airborne transmission. The model is predicting AR through aerosols using the input parameters (infectious) particle emission rates, duration of particle emission, room space volume and exposure time. The model was validated with twelve known outbreaks [11]. For the outbreaks described here the measured particle emission rates were converted to quanta emission rates, where a quantum represents the amount of virus sufficient to infect 63.2% of susceptible persons. With the assumption that the quanta are evenly distributed in the room, the infection risk via aerosol for the two choirs was calculated. The PIRA model does not distinguish between SR and LR transmission but assumes equal exposure of everyone in the entire room to emitted aerosols.

Probability of infection for short-range and long-range exposure

The infection probability depends on the exposure and differs between SR and LR exposed individuals. No model is available to relate the SR infection risk to parameters that were, or could have been, determined from the outbreak investigation. We calculated the additional SR risk originating from the primary cases by statistical inference but cannot relate it to characteristics of the setting or behavior. The LR infection risk, on the other hand, is a mathematical function of the aerosol inhalation dose. The latter function is calculated in 4 steps:

Step 1: Definition of exposure categories

Choir 1: We divided the choir members into those who either had a conversation with the primary case that night or sat within 1.5 m distance (SR exposure) and all others considered as having been subject to LR exposure only.
Choir 2: Analogous to choir 1 we defined SR exposure as having had a conversation with the primary case (the choir director) or having been seated within 1.5 m distance during the rehearsal. The latter

was the case only for the alto singers in the second part of the rehearsal. The rehearsal consisted of a pre-rehearsal with few choir members followed by the main rehearsal with all choir members, thus we stratified the choir members in four groups i) by SR/LR exposure and ii) by participation in both parts or in the second part of the rehearsal only.

Step 2: Separation of the probabilities of infection due to short- and long-range exposure

The probability of infection for those who were exclusively LR exposed was simply the attack rate of this group. Those who had SR exposure were subject to an additional infection risk (SR risk increase) which was calculated as outlined in Supplement A.4. The above stratification of choir 2 complicates the infection probability calculations which are described in Supplement A.5.

Step 3: Particle emission rates of the primary cases and resulting inhalation doses

Based on the measured particle emission rates of the two primary cases, the cumulative particle concentration in the air was calculated assuming temporal voice activity profiles estimated from reconstruction of the course of events. The concentrations depend also on the spontaneous inactivation of virus in aerosol particles and on the ventilation efficiency during the rehearsal breaks. The number of particles inhaled by the other participants depends on the period of their attendance during the respective rehearsal and on their pulmonary ventilation rate. The calculation model is outlined in Supplement A.3.

Step 4: Calculation of the number AP_{50} of inhaled aerosol particles sufficient to infect 50% of exposed

The dose-response relationship between inhaled particle number and probability of infection is only modified by one parameter which can be written as the quantum γ or, alternatively, AP_{50}. Both values necessarily have the same unit as the inhalation doses, i.e., aerosol particles. Supplement A.6 describes the calculation of the quantum γ by statistical inference and its conversion to AP_{50}.
The present AP_{50} estimate is specific to the outbreak strain and the viral load of the primary cases around the day of or one day before symptom onset. To extend the applicability of existing risk models to the variant of concern, B.1.1.7, we propose a dose adaptation estimated from the observed changes in the reproduction number R in Section A.7.

Ethics statement

The study was conducted as outbreak investigation within the framework of the Prevention of Infection Act and thus exempt from submission to an ethical review committee.

Results

Outbreak choir 1

The choir has 96 members, including the choir director and pianist. Eighty-five choir members sent back the questionnaire (89%).
Among them, 38 (45 %) were PCR-positive, and 64 (75 %) were confirmed by serology yielding a total number of 65 (76 %) laboratory-confirmed infections. All PCR-positive choir members with a subsequent serological test seroconverted (n=37).

Identifying date of transmission and primary case (choir 1)

Usually, the choir rehearsed once a week for 2.5 hours with a 15-minute break when windows were tilted for ventilation. Thus, there were rehearsals on 02 March and 09 March 2020. Because of a planned concert of the "Liverpool Oratorio" there was an extra weekend rehearsal that took place on 07 March 2020.

RR was highest for the 09 March rehearsal (Table 1). The PAF for the 09 March rehearsal was 91%, but reached not more than 22% for any of the other rehearsals. All but one choir members with confirmed SARS-CoV-2 infection participated in the 09 March rehearsal and 6 participated only in the 09 March rehearsal, whereas none participated only in one of the 02 or 07 March rehearsals. The one PCR- and seropositive choir member who did not participate in the 09 March rehearsal was living in the same household with another choir member who could have transmitted the virus within the household.

Table 1: Risk ratios of laboratory confirmed SARS-CoV-2 infection for participation in different rehearsals of choir 1, Berlin, March 2020.

Rehearsal	exposed			unexposed			RR	95% CI	p-value
	cases n	total N	AR (%)	cases n	total N	AR (%)			
09 March	64	71	90	1	14	7.1	12.6	1.91-84	<0.001
07 March, am	51	61	84	14	24	58	1.4	1.00-2.1	0.01
07 March, pm	49	60	82	14	23	61	1.3	0.95-1.9	0.05
02 March	52	69	75	12	14	86	0.9	0.68-1.1	0.40

AR=attack rate; RR= risk ratio; CI=confidence interval; am = morning; pm=afternoon

Fourteen choir members reported to have been ill within 10 days before to two days after the rehearsal on 09 March 2020, rendering them potential sources for the outbreak. Of those, 13 were either seronegative, or had no known exposure to a case outside of the choir. Furthermore, they had no travel history to a designated risk area, and none of the indicated disease episodes that began before 09 March included loss of smell or taste. Thus, it appears likely that they were not the source of this outbreak.

The 14th potential source case was briefly ill on 03 and 04 March 2020, with sore throat and diarrhea. After recovery, the case attended a party in another German town approximately 580 km away on 07 March (and missed therefore the rehearsals on that day). Ten participants of that party were reported with COVID-19 and additional 30 were said to have been ill. The choir member became ill on 10 March 2020, with dry cough and high fever above 40 degrees centigrade and was later hospitalized with the need for supplemental oxygen. The son (who had not attended the party) became ill also on 10 March 2020. Sequences of specimens of members of choir 1 and from party members belonged to the same outbreak strain (with one exception; see below, "Sequence typing"). The cases´ symptom onsets show a lognormal distribution with a peak on 12 March 2020, i.e., three days after the rehearsal, resembling a point-source outbreak (Figure 2).

Taken together, the RR, the PAF for individual rehearsals, the evaluation of potential source cases, the distribution of symptom onsets, and the sequence results strongly suggest that choir members became infected on 09 March. The identified likely source/primary case attended a party two days

before the rehearsal, likely shed virus presymptomatically, and infected inadvertently both a family member as well as the choir. The reconstructed seating order of the rehearsal on 09 March 2020 with labeling of the primary case and the infection status is shown in Figure 1.

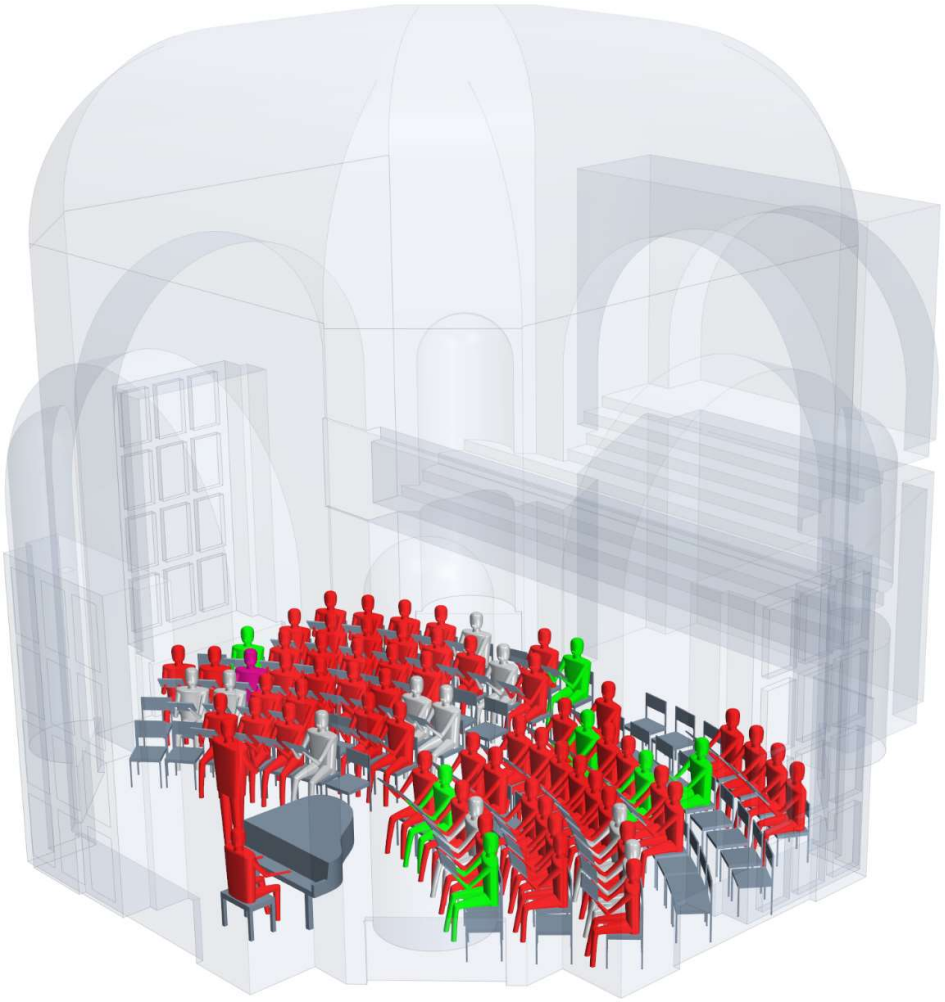

Figure 1. Room model and reconstructed seating order of choir 1, Berlin, 09 March 2020.
Presumable primary case in purple, members with laboratory-confirmed SARS-COV-2-infection in red, SARS-CoV-2 seronegative members in green, members with unknown disease status in grey, standing person = choir director.

Outbreak description (choir 1)

Apart from the presumed source case, 77 choir members were present at the 09 March rehearsal, and 70 (response rate 91 %) sent back the questionnaire. Five fulfilled the described exclusion criteria. Thus, 65 (84%) of 77 were included for further analysis. Of the 65 participants, 58 (89%) were confirmed cases, none was a possible case and 7 (11%) were non-cases (Table 2). Of the 58 confirmed cases, 57 were positive by serology and one was positive only by PCR. Median age of the participants of the 09 March rehearsal was 51 years, 52 years among cases and 45 years among non-cases. Forty-six (71%) were female, similar among cases and non-cases. Whereas the average number of household members was the same in both groups, symptomatic secondary AR was 47 % and laboratory confirmed AR was 25 % among cases, but both were 0 % among non-cases (Table 2).

Table 2: Characteristics of cases (n=58) and non-cases (n=7) of the 09 March rehearsal of choir 1.

	Confirmed cases n (%)	Non-cases n (%)
N	58 (89%)	7 (11%)
PCR-Test (positive/conducted)	35/45 (78%)	0/2 (0%)
Serology (positive/conducted)	57/57 (100%)	0/7 (0%)
Age (median, IQR)	52 (43-60)	45 (32-56)
Gender		
male	17 (29%)	2 (29%)
female	41 (71%)	5 (71%)
Theme / function		
soprano	19 (33%)	1 (14%)
alto	20 (34%)	4 (57%)
tenor	7 (12%)	1 (14%)
bass	10 (17%)	1 (14%)
choir director/pianist	2 (3.4%)	0
No. household members (total)	75	9
ill household members (total, attack rate)	35 (47%)	0 (0%)
lab-confirmed SARS-CoV-2 positive household members (total, attack rate)	19 (25%)	0 (0%)

IQR: Interquartile range

The most frequent symptom was fatigue (79 %), followed by headache (67 %) and cough (57 %; see Supplement table 1). Dyspnea was reported by 31%. Thirteen (22 %) indicated partial loss of smell and 18 (31 %) indicated to have experienced complete loss of smell. Eighteen (31 %) indicated partial, 14 (24 %) complete loss of taste. Disease severity was mild in 39 cases (67%), moderate in 18 (31%, but only one case was diagnosed with pneumonia). One case (1.7 %) was mechanically ventilated (critical, 1.7%). None died.

The mean incubation time was 4 days (range 1-18) with a median and interquartile range (IQR) of 4 days and 3-4 days, respectively (Figure 2). The case with symptom onset 18 days after the rehearsal on 09 March had a positive PCR after 11 days and disease onset after 16 days (5 days later). A household transmission cannot be excluded since the partner was singing in the choir as well and diseased on 10 March. Median duration of illness was 16 days (IQR 10-25).

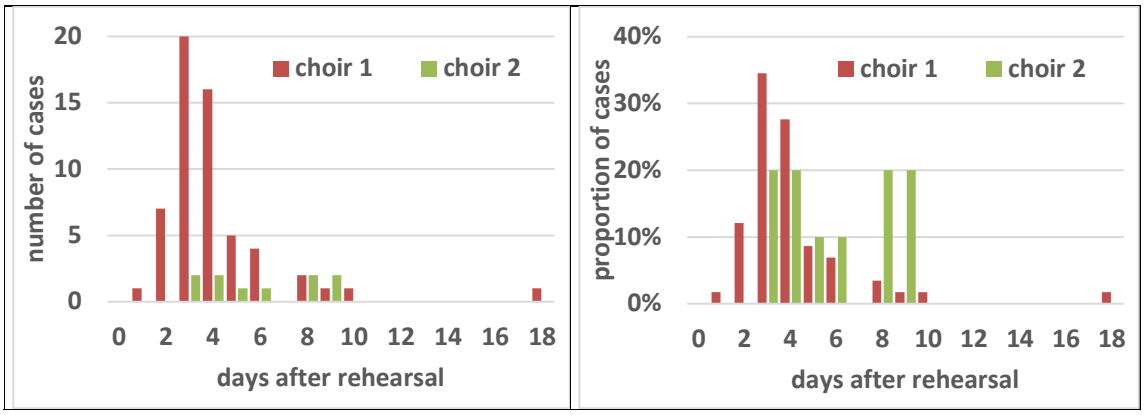

Figure 2. Frequency distribution of cases of choir 1 and 2 by day of symptom onset after the respective rehearsals, Berlin, March 2020. Left: frequency of number of cases, right: proportion of cases.

Outbreak choir 2

The choir director of choir 1 also led the rehearsal of choir 2 on 12 March 2020. He noticed first symptoms of COVID-19 after the rehearsal the same day. Apart from the choir director 42 members of the choir attended the rehearsal. The latter started with a subgroup of 13 individuals forming a chamber choir. The choir director sang the solo part of an aria or accompanied at the grand piano. After 45 minutes, two windows were opened widely for a couple of minutes for ventilation during a pause and additional 29 choir members joined the group. During the following main rehearsal, the director sat mostly at the grand piano but was also leading a discussion standing near the alto singers (Figure 3).

The median age of the choir members was 56 years, the IQR was 51 to 61 years. Twenty-four (57%) of the 42 participants were female. We identified 10 confirmed cases and 32 non-cases for an AR of 24 %, significantly lower than the AR of choir 1 ($p<0.01$). The median incubation period was 5 days (compared to 4 days in choir 1; $p=0.02$; Figure 2).

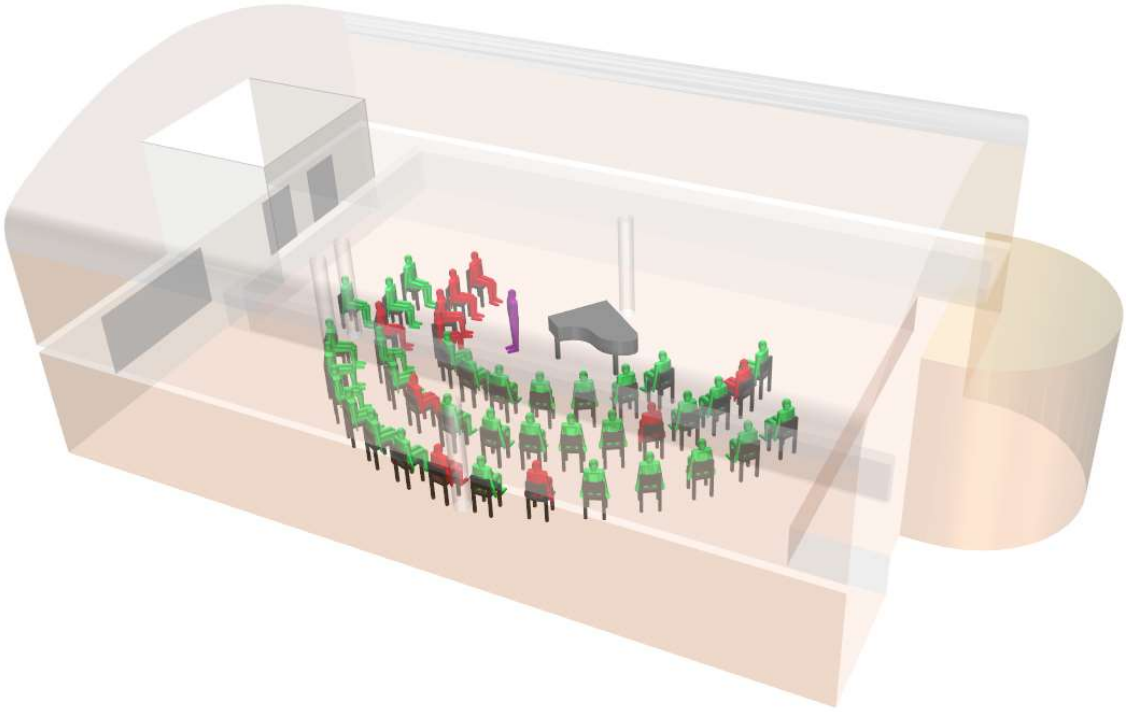

Figure 3. Room model and reconstructed seating order of choir 2, Berlin, 12 March 2020. Presumable primary case in purple, members with laboratory-confirmed SARS-CoV-2-infection in red, members with negative SARS-CoV-2 serostatus or (if not performed) without symptoms in green, standing person = choir director.

Sequence typing

We performed sequencing of three participants of the party which the putative primary case of choir 1 attended, 9 specimens of choir 1 members, one specimen of the choir director and one specimen of a choir 2 member. With the exception of one outlier strain the outbreak strain was found in specimens from all party participants, 9 members of choir 1, including the choir director, and one

member of choir 2 (Supplement table 2). Compared to reference strain Wuhan-Hu-1 (NC_045512.2) we found for all genomes of the outbreak strain 5-6 single nucleotide polymorphisms (SNPs) whereas for the outlier strain EPI_ISL_753799 only 3 SNPs at different locations (Supplement table 2). We identified for the outbreak strain 3, and for the outlier strain 2 synonymous amino acid substitutions (Supplement table 2).

The outlier sequence of a member of choir 1 was aberrant and even belonged to another clade. Phylogenetically, the outbreak strain clusters in GISAID clade 20A, with only one base substitution compared to genomes sampled from Berlin in March 2020. The outlier sequence with only 3 nucleotide substitutions to root strain Wuhan-Hu-1 clusters in GISAID clade 19A (Figure 4).

The patient to whom the outlier strain belonged became ill on 12 March 2020 and was tested positive for SARS-CoV-2 on 15 March 2020. However, she was no likely source of secondary cases at the choir, as her symptom onset was three days after the 09 March rehearsal, and the only secondary case was her husband who fell ill on 22 March.

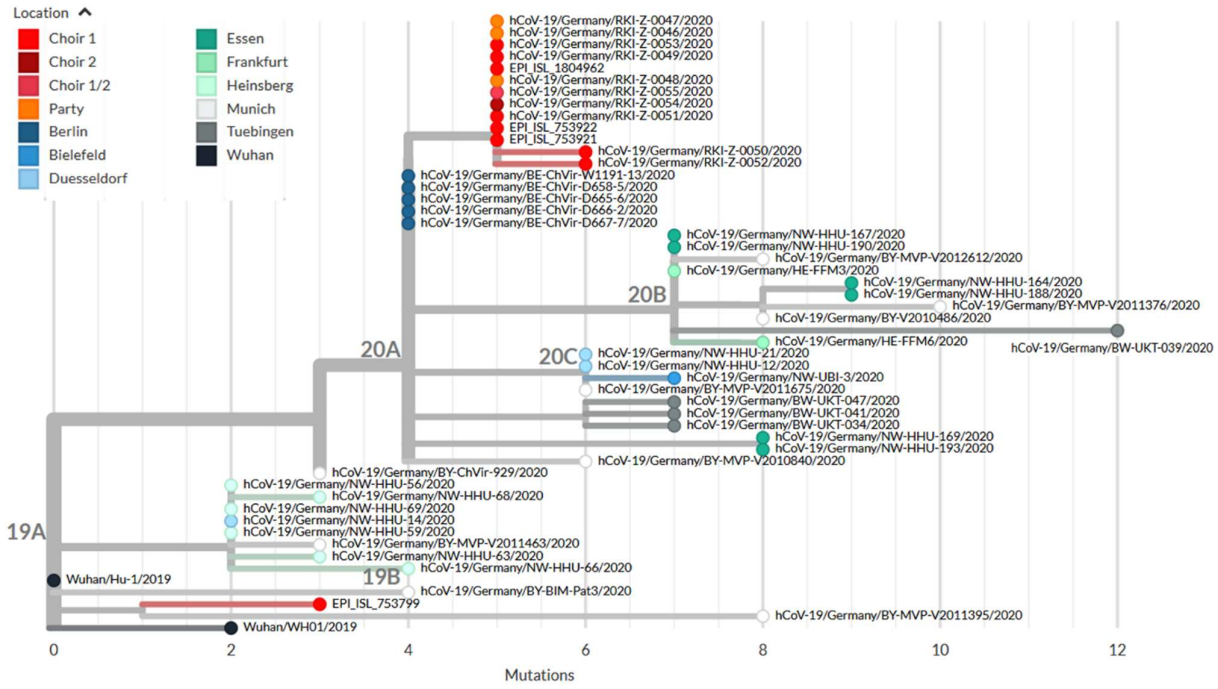

Figure 4: Phylogenetic relationship between the outbreak strain (choir 1, choir 2, party), the aberrant strain (choir 1), and unrelated sequences from different locations in Germany, sampled until end of March 2020. Branch length given as number of mutations.

Sequence of events

It is most likely that the one choir member who had attended the party introduced the SARS-CoV-2 at the choir 1 rehearsal on 09 March 2020 (Figure 5). During this rehearsal the choir director must have acquired the infection and – being the only link to choir 2 - introduced the virus at the rehearsal on 12 March 2020.

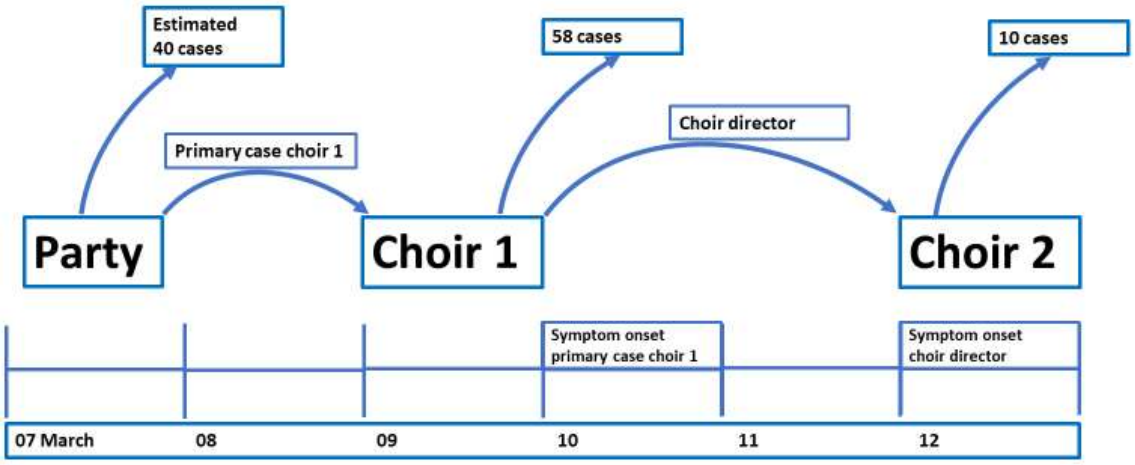

Figure 5. Chronology and number of cases originating from each event, Germany, March 2020.

Particle emission rates

The particle emission rates were lowest for breathing through the nose, higher for speaking and reached substantially higher values when singing (Figure 6). However, the scatter of particle emission rates between single subjects is high. The presumable primary case of choir 1 had a particularly high particle emission rate when singing the "Liverpool Oratorio" (5979 P/s). The emission rate does not seem to correlate with the vocal pitch (Supplement figure 1). Two subjects were excluded because another particle source (e.g., beard, not wearing clothes properly, moving too much) obviously had influenced the measurement.

A repeat measurement on another day showed that the variation of emission rates was higher between individuals than between two measurements of the same individual. The presumable primary case still emitted a high number of particles when singing the "Liverpool Oratory" (2786 P/s) but was not the "top emitter" anymore (Supplement figure 2).

Besides the number, also the size of the particles influences the distribution of the particles in the room. More than 85% of all particles measured were smaller than 1 µm and about 99 % were smaller than 3 µm. All of these are ideal airborne particles, which follow the air flow for a long time.

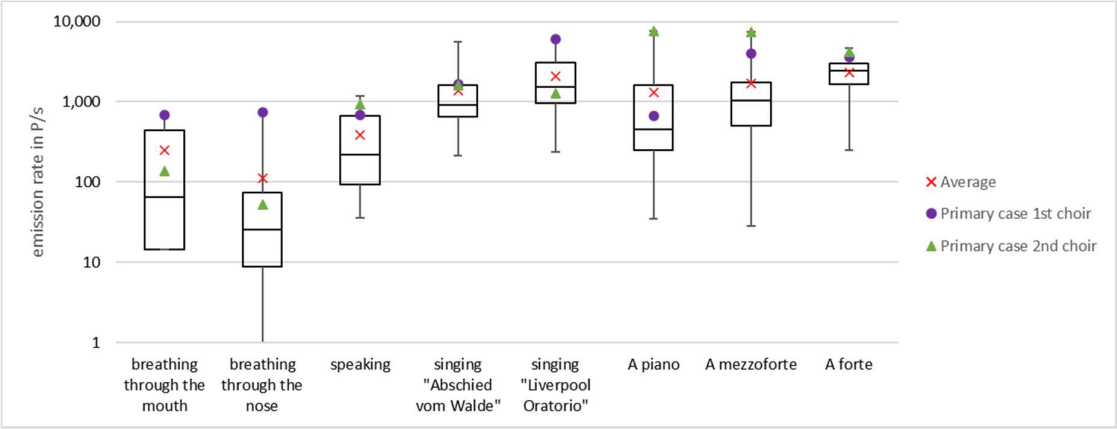

Figure 6. Box plots of cumulative particle emission rates for different activities among members of choir 1 (n=16), Berlin, July-October 2020. Whiskers represent minimum/maximum values. Primary cases of choir 1 and choir 2 are indicated as points or triangles, respectively.

Environmental investigations

The rehearsal of choir 1 took place in a room with a space volume of 1200 m^3. A supply air volume flow of 200 m^3/h was calculated based on the window opening during the rehearsal, the outside temperature (7 °C) and the wind speed (2.5 m/s). The concentration of particles exhaled by the primary case and floating in the air was estimated to have reached up to 10,000 P/m^3 after 2.5 hours, based on the calculations described in Supplement A.3.

The rehearsal of choir 2 took place in a room with a floor area of 234 m^2 and a space volume of 1720m^3. The supply air volume was calculated from the duration of ventilation and the perceived temperature drop in the room. That night the outside temperature was 8 °C, wind speed was 3.5 m/s. In the rehearsal room the concentration of the particles exhaled by the primary case and floating in the air reached up to 1000 P/m^3 after 2.0 hours, according to our model calculation.

The large difference between the particle concentrations was primarily a consequence of the different particle emission rates of the two primary cases (approximately factor 5; Figure 7). Second, the rehearsal of choir 1 was half an hour longer (25%) than that of choir 2. Since inhalation doses increase with up to the square of the exposure duration (at constant emission rate), the latter difference in rehearsal duration yields a risk increase by an approximate factor 1.5. Third, the larger room of choir 2 allowed for better aerosol dilution (approximate factor 1.4). The three factors combine to an approximate ratio of 10 between the inhalation doses of choirs 1 and 2 and a consequent higher attack rate in choir 1.

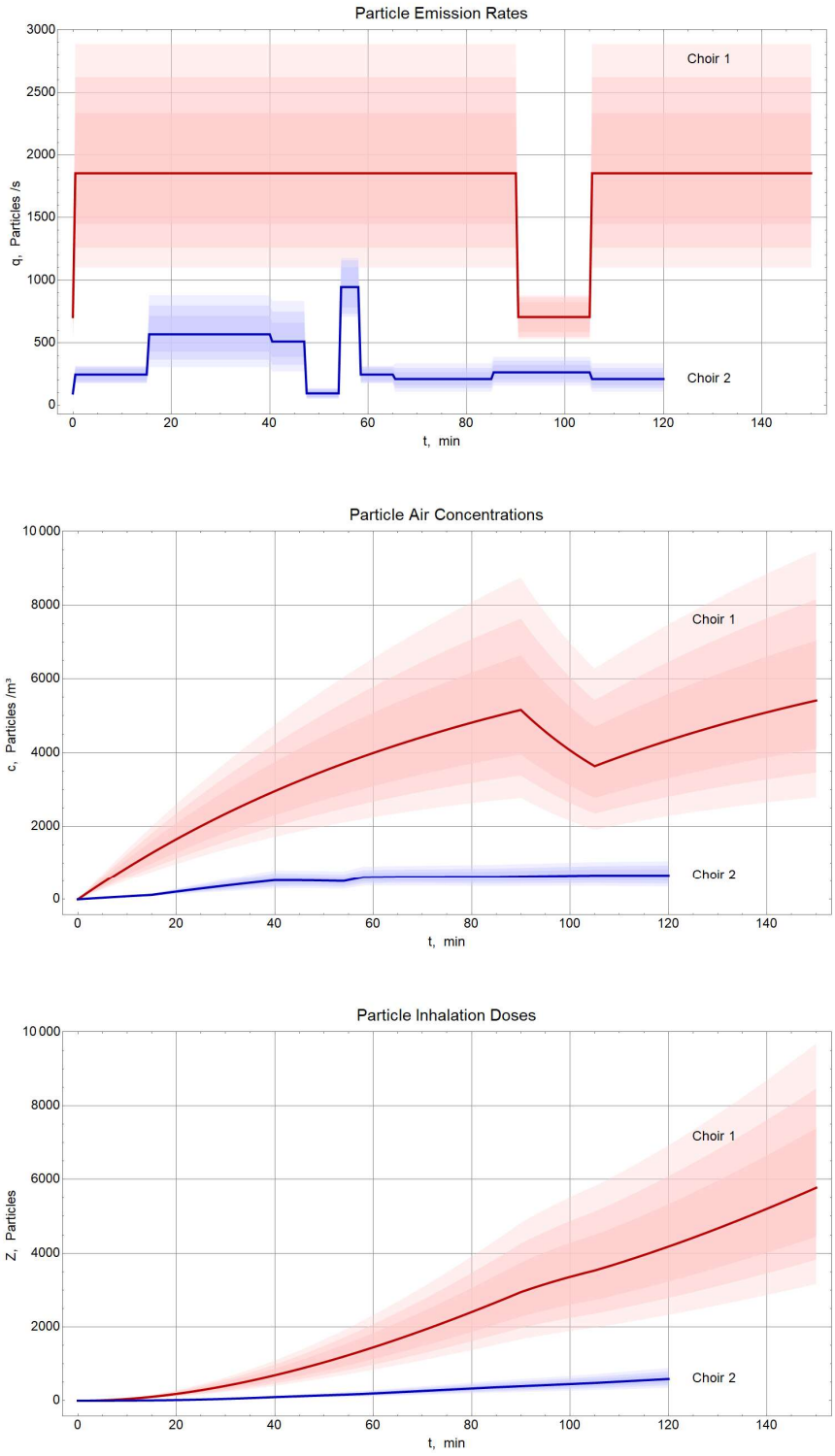

Figure 7: Particle emission rates of the primary cases in both choirs (top), cumulative particle concentration (emitted by the primary cases) in the room air (middle) and resulting inhalation doses (bottom) according to the model calculation described in Supplement A.3, Berlin, March 2020. The shading indicates the uncertainty resulting from parameter estimation, showing the central credibility regions for 68.3%, 90%, and 99% coverage determined by Monte-Carlo simulations. Solid lines indicate the median values.

Predicted infection risk via aerosol (PIRA)

The attack rates predicted by the PIRA model [12] match well the attack rates that actually occurred (Figure 8). For choir 1 a PIRA of 92% were calculated, which is slightly higher than the observed AR of 89%. For choir 2 two different exposures (attending the entire rehearsal vs. attending just the main rehearsal) were evaluated. For the choir members attending the entire rehearsal an AR of 23% was observed and a PIRA of 27% was calculated, whereas for just attending the main rehearsal an AR of 24% was observed and 20% predicted. The PIRA for the entire choir 2 is 22%. Besides the predicted risk of infection under the most likely assumptions (ratios of speaking, singing and breathing, ventilation duration and air volume flow) uncertainty ranges are provided by variation of these parameters.

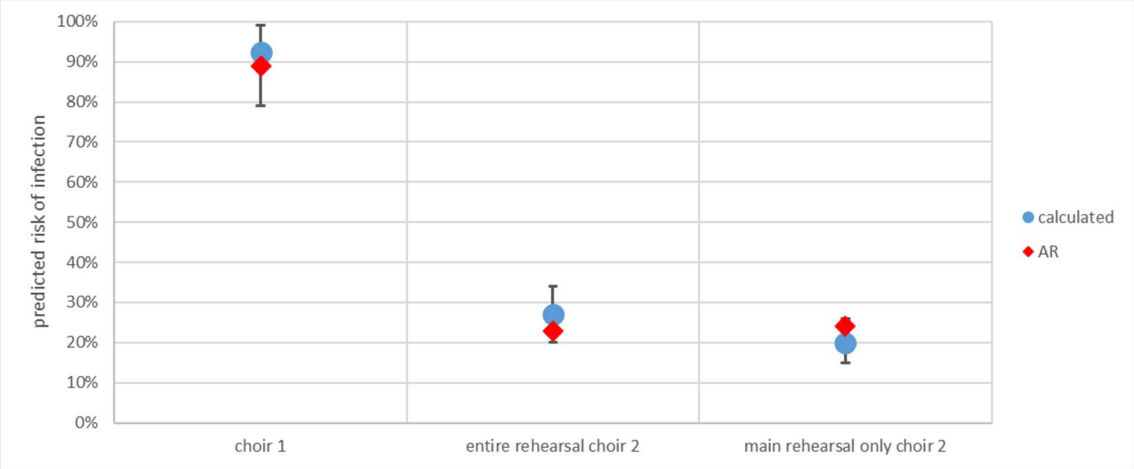

Figure 8. Predicted infection risks for the two rehearsals from the PIRA model [12], Berlin, March 2020. The error bars indicate the uncertainty resulting from parameter estimation

Probability of infection for short-range and long-range exposure

Choir 1: Of the 58 cases, 51 had LR exposure only and 7 had additional SR exposure. Probability of infection by LR exposure was 0.89 (median, 95% CI: 0.80 – 0.95) and with additional SR exposure 0.86 (median, 95% CI: 0.55 – 0.99). The resulting SR risk increase is 0.46 (median, 95% CI: 0.02 – 0.94). The latter estimation has a large CI because LR infection probability is near 90% and the group which is additionally SR exposed is small. This prevents narrow estimation of the SR risk increase, as can be seen from the flat grey curve in Fig. 9.

Choir 2: Of the 10 cases, 4 had LR exposure only whereas 6 had additional SR exposure (Table 4). Probability of infection by LR exposure was 0.18 (median, 95% CI: 0.06 – 0.36) and with additional SR exposure 0.43 (median, 95% CI: 0.20 – 0.68). The resulting SR risk increase is 0.31 (median, 95% CI: 0.04 – 0.62).

The posterior distributions of all probabilities, given the observed cases numbers, are shown in Fig. 9. SR risk increase estimation has high uncertainty since it is backward calculated from estimates of the SR and LR infection probabilities. The large difference in LR infection probability between the two choirs reflects the one order of magnitude difference in the inhalation doses.

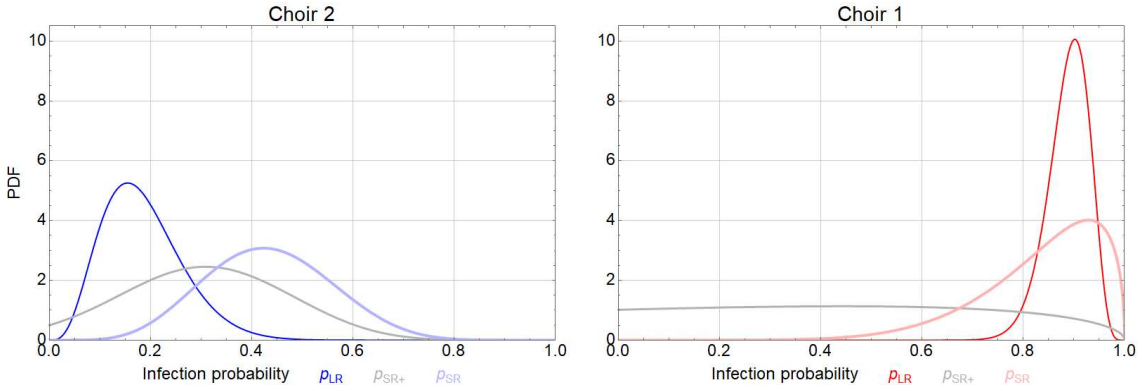

Figure 9. Posterior distributions of the LR, SR increase (SR+), and combined (SR) infection risks in the two choir rehearsals, Berlin, March 2020.

Table 4: Grouping of the members of choir 2 into four cohorts, by SR/LR exposure and by duration of exposure during rehearsal, Berlin, 12 March 2020.

cohort	short-range (SR) / long-range (LR) exposure	participation in the 2 parts of rehearsal	number of choir members	cases	Attack rate (95% CI)
1	SR + LR	both	5	2	40 % (5-85)
2	SR + LR	only second	9	4	44 % (14-79)
3	LR	both	8	1	13 % (0-53)
4	LR	only second	20	3	15 % (3-38)

CI: confidence interval (Clopper-Pearson)

Dose for infection of 50% of the exposed

The combination of the estimated inhalation doses (shown in Fig. 7, bottom) with the estimated related infection probabilities (shown as "LR" curves in Fig. 9) allows inference of the dose-response relationship, as outlined in Supplement A.6. The result is shown in Fig. 10. The parameter γ of the exponential dose-response model (the quantum associated with a 63.2 % AR among susceptible exposed) has a median value of 2497 (95% CI: 1499 – 4159) aerosol particles. The aerosol particle dose associated with infection of 50% of the exposed, AP_{50}, is 1731 (median, 95% CI: 1039 – 2883; Figure 10).

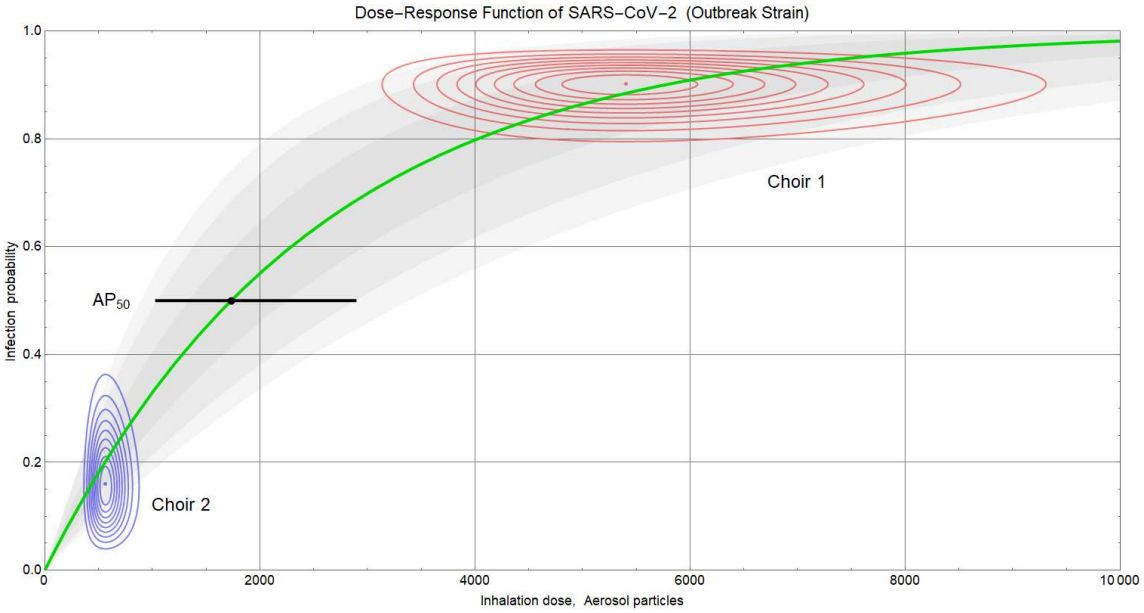

Figure 10. Dose-response relation Eq (8), Supplement A.6, for different values of the quantum γ. Green curve: Median, $\gamma = 2497$ aerosol particles. Gray shaded areas: Central credibility regions for 68.3%, 95%, and 99% coverage. Black marker: Median (1731) and 95% CI (1039 – 2883) of the particle dose leading to infection with 50% probability (AP_{50}). Red and blue contours: Linear equidistant iso-lines of the probability density of pairs (Z, p_{LR}) as inferred from the two choir rehearsals.

Discussion

We report two super-spreading events associated with choir rehearsals. Integrated epidemiological, serological and sequencing data suggest that both outbreaks were connected and were each, initiated by single primary cases. One primary case transmitted presymptomatically. The two events differed in their primary cases´ particle emission rates and duration, room space volume, and exposure time of the choir members, resulting in different probabilities of infection through LR exposure and attack rates. Incorporating these parameters in the Predicted Infection Risk for Aerosol Transmission (PIRA) model, attack rates in both choirs could be predicted with high accuracy.

It was a challenge to identify the date of infection as well as the primary case for choir 1 out of three possible rehearsals with 96 participants. However, analysis of the relative risks and population attributable fraction and the timing of symptom onsets with respect to the rehearsals pointed clearly towards the rehearsal on 09 March 2020 as the day of infection. Identical sequence results from the choir members and participants at the party, which was also attended by the presumed primary case, further corroborated the identification of the date of infection, as well as the primary case.

In contrast to the median incubation time of 5 days in choir 2 the median incubation time of 4 days in choir 1 is somewhat shorter than the usually reported incubation period of 5-6 days [12, 13]. Given that higher viral load is associated with a lower incubation period [14], the data from the two outbreaks suggest that the inhalational dose exposing the choir members was substantially higher in choir 1 than in choir 2. This is unambiguously predicted by our model calculations displayed in Fig. 7 and concurs with the findings from the Skagit choir outbreak where the median incubation period was 3 days and the attack rate of 87% was as high as in choir 1 [2].

Adding the party attended by the primary case of choir 1, we report three super-spreading events occurring within a period of 6 days. For two of them we have described the conditions clearly. As Buonanno pointed out a super-spreading event does not necessarily require the "rare presence of a superspreader" as long as the co-existence of 'favourable' conditions coincide [15]. The two outbreaks demonstrate quite convincingly the risk of SARS-CoV-2 infection due to indoor singing during the pandemic. The primary case in choir 1 was asymptomatic on the day of the rehearsal. Thus, allowing rehearsal participation based on absence of symptoms would not have prevented this outbreak. As singing emits approximately 30 times more particles than talking or breathing, the presence of an infectious person singing in a room can be equaled to the presence of 30 infectious persons talking or breathing. The other singers in the room likely aggravated the situation by contributing to the mixing of the room air more rapidly.

The total particle emission of the primary case was higher in choir 1 since the primary case was singing most of the time and the rehearsal lasted 30 minutes longer. Furthermore, the rehearsal room of choir 1 was 30% smaller in volume than the one of choir 2, leading to a higher accumulated particle concentration. In consequence, the infection probability through LR exposure was 5 times higher in choir 1. The additional SR risk increase in choir 1 could not be recovered due to the small difference in the attack rates between those with LR exposure only and those with both SR and LR exposure.

It is a strength of this analysis that the two rehearsals of choir 1 and 2 build on a rare case of the same SARS-CoV-2 strain having caused two well documented outbreaks with significantly different attack rates. Thus, two well separated points of the dose-response function were observed which allows to construct the dose-response relationship of LR exposure and probability of infection with unprecedented accuracy (Figure 10).

The infectious dose refers to particle concentrations, which we derived from particle emission measurements of the primary cases after having recovered. We estimated the number of inhaled particles, previously emitted by the primary case, for a 50% infection rate as 1731 particles. The proportion of infectious particles (virions) in this aerosol is unknown and goes beyond the scope of this article.

The PIRA model [11] developed by one of the authors (MK) was used to estimate the expected number of infected persons and predicted the actual number well. The same model estimates that - given the conditions of choir 1 - a rehearsal of 7 minutes would have led to an attack rate of about 1.5 %, thus, the first person out of 80 would be expected to be infected after 7 minutes into the rehearsal. For a rehearsal of 15 min the air volume flow should have been 500 $m^3/(h*person)$ to prevent infections from happening, which is about 10 times the air volume flow required to keep the CO_2-level at, or below, 1000 ppm. Volume flows like this are not achievable by ventilation through windows. Solely large concert halls with mechanical ventilation and with a clearly reduced number of visitors might offer such high-volume flows per person, as well as outdoor rehearsals.

On a side, our data demonstrate the limitations of CO_2-measurements that are frequently used in an attempt to gauge the infection risk for indoor settings. A person singing would produce little more CO_2 than a person breathing or talking. However, the numbers of particles emitted will vary drastically.

We acknowledge the following limitations. First, as we measured seropositivity in choir members approximately 3.5 months and 6.5 months after the event, it is possible that we attributed some to the outbreak, which were infected later and through a different transmission event. However, as cases diseased following the rehearsal and seroprevalence in German regions did not exceed 1.2% after the first wave [16], the risk that we falsely attributed cases to the outbreak is small. Second, particle emission was measured when primary cases had recovered from disease. Particle emission may be substantially higher when persons are diseased [17]. This would result in a higher estimated number of (partially infectious) particles necessary to infect 50% of exposed (AP_{50}). Third, the primary cases participated in the transmission events one day before or on the day of symptom onset, when viral load peaks [18]. Lower viral loads would result in lower infection risks and a higher $AP_{50.}$ Fourth, calculations apply to the outbreak strain and would need adjustment for other variants. Given the higher infectivity of currently circulating variants of concern (VOC), adjustment for the VOCs would most probably result in a higher infection risk and lower AP_{50}. We propose an adjustment of AP_{50} for B.1.1.7/VOC202012/01 in Supplement A.7.

Conclusion

Our investigation demonstrates the risk of LR exposure, which accumulates rapidly with increasing duration. Through LR exposure, an infectious person may have generated first infections after only a few minutes of singing, even under room conditions large enough to accommodate a choir. Because of the potential for presymptomatic infectiousness, greatest caution is needed in indoor, aerosol-accumulating settings.

Acknowledgements

Anna Stoliaroff-Pépin for help with taking blood samples; Viktoria Streib and Hanna Töpfer for administrative assistance; Magdalena Simstich and Corinna Fruth for entering data; Romy Hildebrandt (Kreisverwaltung Mainz-Bingen, Amt für Gesundheitswesen), Florian Burckhardt (State Health Department Rhineland-Palatinate) as well as Manfred Vogt, Monika Cremer-Kahn and Benedikt Frei (Landesuntersuchungsamt, Institut für Hygiene und Infektionsschutz, Koblenz) for investigating and providing specimens from the party outbreak, Julia Lange, Hansjörg Rotheudt, Lukas Schumann from the Hermann-Rietschel-Institute (for help in particle measurements), Eugen Lichtner, Kevin Lausch from the Hermann-Rietschel-Institute (for setting up the models for the seating order), Clemens Bodenstein, Caroline Eberle, Juliane Fraissinet, Melanie Hoffmeister, Bianca Hube, Silvia Muschter, Therese Muzeniek, Stefanie Schürer, Franziska Schwarz, Anette Teichmann and Julia Tesch (Robert Koch Institute) for support with serological testing, Steven Uddin and Ute Kramer (Robert Koch Institute) for sequencing and Jan Walter (Robert Koch Institute) for valuable comments on the manuscript.

Supplement

A.1 Neutralization Test

Sera were diluted in DMEM (10 % FCS, 2 mM Glutamine) in six two-fold dilutions resulting in dilutions of 1:10 up to 1:320. These dilutions were mixed 1:1 with SARS-CoV-2 (strain BetaCoV/Germany/BavPat1/2020, kindly provided by Dr. Roman Woelfel, Institute for Microbiology of the German armed forces ("Institut für Mikrobiologie der Bundeswehr")), final virus concentration 1,000 $TCID_{50}$ /mL and incubated at room temperature for 1 h. Subsequently, 100 µL of diluted serum-virus mix were added to wells containing 2 x 10^4 Vero E6 cells/well (#85020206, European Collection of Authenticated Cell Cultures (ECACC), Porton Down, UK), in a 96-well plate. Each sample dilution was tested in eight replicates and cells were incubated for 5 days (37°C + 5 % CO_2). Positive (cytopathic effect visible in light microscopy) and negative wells were counted and $PRNT_{50}$ values calculated according to Reed and Muench [19]. A positive control consisting of a known positive sample was analyzed in parallel and back-titration of the virus stock was performed for quality control.

A.2 Sequence typing

For Illumina Sequencing, RNA was extracted using the MagNApur 96 DNA and viral NA small volume Kit (Roche) on a MagNA Pure 96 System as recommended by the manufacturer. Sequencing was done by applying an amplicon-based sequencing approach using the 600-cycle MiSeq reagent v3 cartridge (Illumina) as described before [20]. Consensus sequence determination was done by reference by using bowtie2 version 2.3.5.1 for mapping, GATK MarkDuplicatesSpark version 4.1.4.1, for elimination of read duplicates, and by using bcftools [20].

For MinION Sequencing RNA was extracted using the QIAamp viral RNA kit (Qiagen, Hilden, Germany) in a total volume of 100 µl and transcribed to cDNA using the Superscript IV reverse transcriptase (Thermo Fisher Scientific, Darmstadt, Germany). Whole genome sequencing of the samples was performed after previous specific whole genome amplification of SARS-CoV-2 (Brinkmann et. al, manuscript in review). The libraries were prepared using the Ligation Sequencing Kit LSK-109 and loaded on Oxford Nanopore MinION SpotON Flow Cells, FLO-MIN106D, R9.4.1 (Oxford Nanopore Technologies). For transcription to FastQ sequences, computational separation of barcodes and preparation of alignments Guppy v.3.4.5 for Windows with standard parameters was used. Resulting contigs were handled with Geneious Prime 2.1 and used for calculation of accuracy and genome coverage of the consensus sequences. SNP calling was performed only on genome regions with a coverage of reads > 10 and a frequency of > 65 %.

A.3 Calculation of particle inhalation doses

The (infectious) aerosol doses inhaled by the rehearsal participants have not been measured and need to be estimated. The general approach is to estimate the emission, distribution, removal, and

inhalation of infectious matter using physical models. In this section we calculate probability distributions of the number Z of aerosol particles inhaled by rehearsal participants.

Particle emission rates

The emission of virus-laden particles is estimated from the temporal profile of voice activity of the respective primary case. The activity levels considered are breathing (no voice activity, 0), talking (1), and singing (2). The related particle emission rates of the primary cases have been measured weeks later under controlled conditions and are summarized in Fig. 6. This allows to translate the activity level a = 0, 1, 2 into experimentally determined particle emission rates, $q(\tau)$, at any point τ in time.

The temporal voice activity profile, $a(\tau)$, is estimated from reconstructions of the course of events. For choir 2, these are based on interviews and knowledge of the working style of the choir director. The rehearsals are subdivided into periods of constant activity $a(\tau)$. During most periods a mixture of activities is assumed, e.g., of 0 and 2 during singing parts. The mixing weights are estimated based on knowledge of the two choirs and the pieces sung. The mixing is treated as leading to constant, mean emission rates are calculated by linear combination of measured rates.

In summary, the temporal particle emissions of the two primary cases, $q_1(\tau)$ and $q_2(\tau)$, are estimated based on detailed knowledge of rehearsals 1 and 2 and experimental data shown in Fig. 6. The results are shown in the top row of Fig. 7.

Distribution and removal of particles

The spatial distribution of aerosol particles by convection with ambient air is treated by the common assumption of well-mixed room air [8]. Neglecting finite drift velocities and potential local variations in air flow, aerosol is treated like a (more than) perfect gas instantly reaching uniform concentrations depending only on time.

This limitation of our model could be overcome by computational fluid dynamic (CFD) simulation, which is planned to be implemented. CFD models are more realistic, including the strong dependence on initial and boundary conditions. In real life scenarios like the choir rehearsals, the convolution of uncertainties may gamble away the advantage of higher accuracy, while the expense of CFD prevents Monte Carlo simulation to account for accidental parameter variation. Therefore, we adopt here the seemingly simplistic well-mixed air assumption.

The air concentration of potentially infectious particles emitted by the primary cases, $c(\tau)$, is obtained through weighing up emission against dilution by non-contaminated air during the rehearsal breaks and spontaneous deactivation of virions on aerosol particles. The latter process converts initially infectious particles into harmless matter not contributing to c. The decay of cytopathic active virus titer on airborne particles has been found to be exponential with a half-life of δ = 1.15 h (median) [21].

The temporal evolution of c is described by

$$\frac{\mathrm{d}}{\mathrm{d}\tau}c(\tau) = \frac{q(\tau)}{V} - \left[L(\tau) + \frac{\ln 2}{\delta}\right]c(\tau) \qquad \text{(Eq 1)}$$

with the initial condition $c(0) = 0$. L is the air change rate (unit: h^{-1}) and V is the room space volume in m^3. Time has unit h, emission rates are given in aerosol particles per hour, concentration is obtained in aerosol particles per m^3 by solving Eq (1). The result is shown in the middle row of Fig. 7.

Inhaled particle doses

The inhalation dose is the amount of (partially infectious) aerosol particles inhaled during the rehearsal:

$$Z = \int_{t_{\text{begin}}}^{t_{\text{end}}} A(\tau)\, c(\tau)\, \mathrm{d}\tau \qquad \text{(Eq 2)}$$

where $A(\tau)$ is the pulmonary ventilation rate of the susceptible person. It is assumed as 0.65 m^3/h when singing and 0.54 m^3/h otherwise [12].

The rehearsal of choir 1 was attended by all participants during the entire duration, $t_{\text{begin}} = 0$ and $t_{\text{end}} = 2.5$ h. The rehearsal of choir 2 was split in two parts: The first was attended by 13 exposed persons. The second part was attended by these 13 persons and 29 further persons, 42 in total. The first group was exposed in the period from $t_{\text{begin}} = 0$ to $t_{\text{end}} = 2.0$ h and the second group from $t_{\text{begin}} = 0.833$ h to $t_{\text{end}} = 2.0$ h. This leads to different inhalation doses for cohorts 1 and 3 (attendance of entire rehearsal) versus cohorts 2 and 4 (attendance of second part only) in Table 4. The inhalation doses for both choirs for $t_{\text{begin}} = 0$ are shown in the bottom row of Fig. 7 as functions $Z(t_{\text{end}})$. The lower doses of choir 2, cohorts 2 and 4, are not shown, they are estimated to be 26% smaller than those for cohorts 1 and 3 at $t_{\text{end}} = 2.0$ h.

The accuracy of such calculations is limited by the need to estimate parameters of Eq (1), namely the varying degree of emission, $q(t)$, the duration and effectiveness of ventilation, $L(t)$, and viral half-life δ. For those parameters, plausible ranges were determined while the actual values remain unknown. We assume δ to vary between 0.64 and 1.64 h [21]. The emission rate was modeled using 4 and 7 numerical parameters for choir 1 and choir 2, respectively. Air change rates L during the breaks were estimated from environmental considerations.

It is impossible to determine the actual inhalation doses $Z_{1,2}$ during the two rehearsals, but they may be assumed being random draws from a lognormal, prior probability distribution. This assumption reflects the fact that $Z_{1,2}$ is influenced by several situation-dependent parameters being statistically independent. Assuming that each one is uniformly distributed within its plausibility range leads to a lognormal distribution of Z. The densities of $Z_{1,2}$ were calculated by Monte Carlo simulation with 100.000 random parameter sets, each, and are shown in the bottom row of Fig. 7.

The possibly intuitive ansatz that Z is uniformly distributed within an uncertainty interval leads to a paradox since one cannot be sure the interval bounds were chosen correctly. It introduces an indeterminate error probability that the actual dose lies outside the interval, hence – in contradiction to the assumption – the probability density is not zero outside that interval. The more plausible lognormal distribution avoids this peculiarity and allows calculation of credibility limits for given significance levels. We obtain $Z_1 = 5761$ aerosol particles (median, 95% CI: 3505 – 9470) for choir 1, $Z_3 = 588$ (95% CI: 393 – 879) for choir 2, cohort 3, and $Z_4 = 442$ (95% CI: 291 – 672) for cohort 4.

A.4 Separation of short and long-range infection probabilities

The model assumption of a permanent homogenous aerosol concentration in the room air entails independence of LR aerosol inhalation doses of the position of a given person in the room. The reach of aerosol (transmission) is the room size and denoted here as LR. LR exposure depends on the period of stay within contaminated air. It produces a spatially uniform, inevitable base level of infection risk monotonously increasing over time. Outdoor, LR infection risk converges to zero due to virtually infinite aerosol dilution.

Any circumstance increasing the infection risk above the LR level is denoted as short-range risk increase (SR+). The infection risk for persons exposed through SR is a composite of LR and SR+ risks. If we assign the infection probabilities p_{SR+} to the additional short-range and p_{LR} to the long-range exposure, the probability of infection for persons exposed through SR exposure is

$$p_{SR} = 1 - (1 - p_{LR})(1 - p_{SR+}) \qquad \text{(Eq 3).}$$

$1\text{-}p_{SR}$ is the probability of not being infected, neither by the LR base exposure, nor by the additional SR hazard. For persons without SR exposure $p_{SR+} = 0$, thus $p_{SR} = p_{LR}$.

In the SR of an infectious person larger exhaled droplets may carry pathogens in amounts exceeding the aerosol load by orders of magnitude. Transmission occurs in an unpredictable, discontinuous fashion and may be more dependent on the distance than on the contact time. Therefore, our SR cohort definition involves the seat position and a Boolean indicator for conversations with the primary case while neglecting the conversation length.

The mechanism of SR infection renders it deterministic with hidden variables, rather than stochastic. Probabilistic treatment partly disguises absence of knowledge as random. In that sense, Eq (3) is formal. It allows to estimate p_{SR+} from SR cohort attack rates with the caveat that SR exposure is not a repeatable random process with uniform or constant “success” probability. This applies only to LR infection.

Therefore, the derivation of the dose-response relationship in Supplement A.6 involves only LR cohorts of the two choirs whose attack rates are distributed around p_{LR}. It is possible to include SR cohorts, but not advantageous: Eq. (3) leads to bivariate likelihood functions of (p_{LR}, p_{SR+}) which are difficult to unravel, whereas p_{SR+} eventually is a byproduct. Therefore, the nuisance parameter p_{SR+} is eliminated from the estimation of p_{LR}.

Previous outbreak investigations did not divide the susceptible population into LR and SR cohorts which impairs accurate estimation of the aerosol transmission risk.

A.5 Infection probability distributions

The dose-response relationship of SARS-CoV-2 is calculated by Bayesian inference starting with objective priors [22]. In this section we calculate posterior densities, point estimates, and credibility intervals of the infection probabilities defined above.

In choir 1, out of s_1 = 57 participants with only LR exposure c_1 = 51 have been infected. The case number c_1 depends on the unknown LR infection probability p_1 according to the binomial distribution. The posterior density of p_1 given the observation (s_1, c_1) is obtained via Bayes' rule using the objective (Jeffreys) prior

$$g(p_1) \propto 1/\sqrt{p_1\,(1-p_1)} \qquad \text{(Eq 4)}$$

and is the beta distribution with shape parameters ($1/2+c_1$ = 51.5, $1/2+s_1$-c_1 = 6.5). The 2.5% and 97.5% quantiles of the beta (51.5, 6.5) distribution bound the central 95% credibility interval of p_1.

As point estimate we use the median, throughout this work, for two reasons: The probabilities of over- and underestimation are equal, and the central credibility interval contains the median for any given error probability. The median generally differs from the most likely value (mode), so that the present point estimates may differ from attack rates given in Tables 1 and 4. For p_1 we obtain the point estimate 0.89 (median) and the 95% CI 0.80 – 0.95. The Bayesian credibility intervals are narrower than the Clopper-Pearson intervals given in Table 4.

The situation in choir 2 is complicated by the existence of two LR exposure cohorts, 3 and 4, whose inhalation doses and, thus, infection probabilities are correlated. The low attack rates indicate approximate proportionality between dose and response in Eq (8). Hence, the ratio between the LR infection probabilities p_3 and p_4 approximately equals that of the inhalation doses Z_3 and Z_4.

While the Monte-Carlo simulation (Supplement A.3) produced large variances for both Z_3 and Z_4 it yields a narrow 95% CI (0.710 – 0.784) for the ratio

$$0.753 \approx \frac{Z_4}{Z_3} \approx \frac{p_4}{p_3} = \xi = 0.770 \qquad \text{(Eq 5)}$$

so that p_4 can be replaced by $\xi\, p_3$. We define p_{LR} as being p_3 and obtain the likelihood function

$$l(p_{\mathrm{LR}}) = \binom{s_3}{c_3}\binom{s_4}{c_4} p_{\mathrm{LR}}{}^{c_3}(1-p_{\mathrm{LR}})^{s_3-c_3}(\xi\, p_{\mathrm{LR}})^{c_4}(1-\xi\, p_{LR})^{s_4-c_4} \qquad \text{(Eq 6)}$$

with c_3 = 1, s_3 = 8, c_4 = 3, and s_4 = 20. The Jeffreys prior for Eq. (6) is

$$g(p_{\mathrm{LR}}) \propto \sqrt{\frac{s_3(1-\xi\, p_{\mathrm{LR}}) + \xi(1-p_{\mathrm{LR}})s_4}{(1-p_{\mathrm{LR}})\, p_{LR}\, (1-\xi\, p_{\mathrm{LR}})}} \qquad \text{(Eq 7)}$$

and is equivalent to Eq. (4) for ξ = 1. The posterior distribution of p_{LR} approximates a beta (4.38, 19.42) distribution with high accuracy (Euclidean distance 0.009 between densities). This beta distribution represents a fictitious rehearsal of 120 minutes duration with 23 participants, four of which were infected. We introduce p_2 having the latter distribution as the LR infection probability for choir 2 and $Z_2 = Z_3$ as associated inhalation dose. Thus, p_2 = 0.18 (95% CI: 0.06 – 0.36).

In analogy, the infection probabilities Eq (3) for persons exposed through SR are calculated from the observations in the SR cohorts. For choir 1, p_{SR}= 0.86 (95% CI: 0.55 – 0.99) and for choir 2, p_{SR}= 0.43 (95% CI: 0.20 – 0.68).

The SR risk increase p_{SR+} is calculated from the joint density of p_{SR} and p_{LR}. For choir 1, p_{SR+}= 0.46 (95% CI: 0.02 – 0.94) and for choir 2, p_{SR+}= 0.31 (95% CI: 0.04 – 0.62). The densities of all probabilities are shown in Fig. 9.

A.6 Dose-response relationship

The exponential dose-response model [23] has been found to be appropriate for SARS-CoV [24] and is adopted here for SARS-CoV-2. It relates the probability p of infection to the inhalation dose of pathogens, Z, by

$$p = 1 - \mathrm{e}^{-Z/\gamma} \qquad \text{(Eq 8)}$$

where γ is the dose causing infection with 63.2% probability and is referred to as quantum [8, 11]. The dose-response function, Eq (8), is completely known if γ is known. Z and γ necessarily have the same unit, but the latter is free to choose. In this section we estimate γ as number of aerosol particles.

In Section A.3 we derived probability distributions of the inhalation doses Z_1, Z_2 and in Section A.5 distributions of the related infection probabilities p_1, p_2. The four distributions represent estimation uncertainty, resulting either from incomplete knowledge of parameters (Z) or from finite accuracy of observation (p_{LR}). The uncertainties of Z and p_{LR} are statistically independent, despite the actual values of Z and p_{LR} being correlated by Eq 8). Therefore, the joint density of pairs (Z, p_{LR}) is the product of the densities of Z (lognormal) and p_{LR} (beta distribution). The joint densities for both rehearsals are shown as contour plots in Fig. 10.

Given a pair (Z, p_{LR}), γ is obtained by solving Eq (8):

$$\gamma'(Z, p_{LR}) = -Z / \ln(1 - p_{LR}) \qquad \text{(Eq 9).}$$

The distribution function of γ is the integral of the density of (Z, p_{LR}) over the region $\gamma'(Z, p_{LR}) \leq \gamma$, and derivation with respect to γ yields its likelihood l:

$$l(\gamma) \propto \frac{\mathrm{d}}{\mathrm{d}\gamma} \int_0^{\infty} \int_{1-\mathrm{e}^{-Z/\gamma}}^{1} p_{LR}{}^{c-\frac{1}{2}} (1 - p_{LR})^{s-c-\frac{1}{2}} Z^{\frac{2\mu - \ln}{2\sigma^2}-1} \, dp_{LR} \, dZ \qquad \text{(Eq 10).}$$

Each of the pairs (Z_1, p_1) and (Z_2, p_2) generates such a likelihood function, $l_1(\gamma)$ and $l_2(\gamma)$, for the respective rehearsal. The overall likelihood of γ, given the observations from both rehearsals, is the product of the two likelihood functions:

$$l(\gamma) = l_1(\gamma)\, l_2(\gamma) \qquad \text{(Eq 11).}$$

The function $l(\gamma)$ can be well approximated by a lognormal density with μ = 7.823 and σ = 0.260, which reflects the fact that γ itself is a dose. The interesting parameter of $l(\gamma)$ is its median, our point estimate for γ. Since $l(\gamma)$ appears to be lognormal the median is e^{μ}. The posterior density of the location parameter μ is obtained using Bayes' rule with an objective prior. The univariate Jeffreys

prior for a lognormal distribution with known variance is flat, hence the posterior density of e^{μ} is identical with the likelihood function of γ [25]. For the quantum we obtain γ = 2497 (median, 95% CI: 1499 – 4159) aerosol particles. The most likely value (mode) is 2334 aerosol particles.

The median value is 3% smaller than the quantum value previously assumed in the PIRA model [12], 2586 aerosol particles. PIRA reproduces with remarkable accuracy the attack rates of a dozen documented COVID-19 outbreaks, including the one in choir 1. Our present analysis including choir 2 corroborates the previous estimation of γ and adds its probability distribution and credibility range.

The aerosol particle dose leading to infection with 50% probability, AP_{50}, is proportional to the quantum γ by the factor $\ln 2$. Hence, the distribution of γ is easily transformed into the distribution of AP_{50}which is lognormal with μ = 7.456 and σ = 0.260, AP50 = 1731 (median, 95% CI: 1039 – 2883). The aerosol particles´ equilibrium diameters (after desiccation) are ≥ 0.3 µm. Such particles have diameters below 5 µm and most of them are droplet nuclei.

A.7 Adjustment for lineage VOC 202012/01

Present knowledge of the lineage VOC 202012/01 (B.1.1.7) allows for the possibility that the observed increase of the associated effective reproduction number R_{eff} over the non-VOC lineages is primarily a result of increased transmissibility, rather than of changes of the contact behavior or duration of infectiousness.

Today, an additive increase in R_{eff} appears as plausible as a multiplicative increase. The first might reflect increases in transmissibility in specific subpopulations or contexts while the latter would be expected if transmissibility had increased in all settings and individuals [26]. In this case a higher intrinsic infectiousness of VOC B.1.1.7 would likely be the cause of the increased R_{eff} [27]. Notably, three genetic changes have been found in VOC B.1.1.7 which are thought to result in lower infectious doses [28].

Based on this assumption, AP_{50} for VOC B.1.1.7 can be estimated from AP_{50} for the non-VOC lineage examined here. If both lineages, VOC B.1.1.7 and non-VOC, exhibit the same durations of infectiousness and average rates of contact between infected and susceptible individuals, the ratio between the R_{eff} numbers is the same as the ratio between the transmission probabilities [29].

No indication has been reported that higher infection probability associated with VOC B.1.1.7 was due to different transmission situations or behavior of exposed individuals. A study [28] found no evidence that the increased infection rates were mediated through higher viral loads. Since no higher mean intake doses should be assumed, AP_{50} for VOC B.1.1.7 infection is expected to be smaller.

Infection probabilities in average single transmission settings are small and thus approximately proportional to the doses transmitted, and inversely proportional to AP_{50}. Hence, the AP_{50} values of the VOC B.1.1.7 and non-VOC lineages differ by the reciprocal of the R_{eff} ratio.

Three independent estimations of the increase factor of R_{eff} have been proposed [26, 27, 30]. We calculate the intersection of the three published credibility intervals from a posterior density obtained by multiplication of three associated likelihood functions, analogous to Eq (11). For each published set of a mean estimate and a 95% CI we calculate a lognormal likelihood function as an optimal fit to those parameters. The product of these three likelihood functions is lognormal, too, and represents the combined likelihood of the increase factor. As in the case of γ above, the latter function is the posterior density of the median estimate, given the results of the three studies. We obtain a multiplicative increase of R_{eff} by 1.48 as point estimate and the central 95% CI 1.26 – 1.75 from the 2.5% and 97.5% quantiles. The four likelihood functions are displayed in Fig. 11.

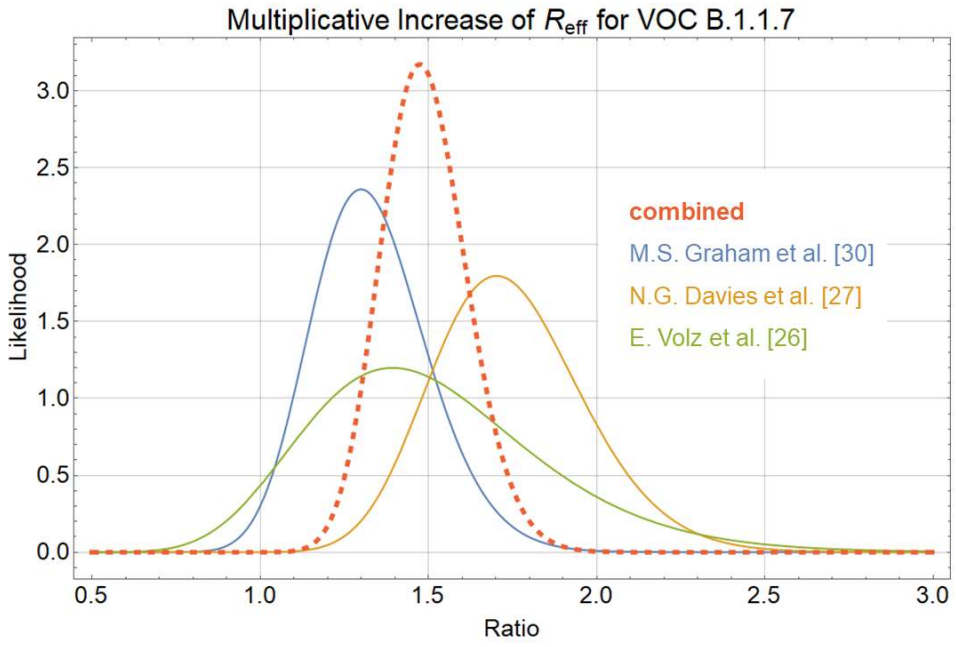

Figure 11. Lognormal likelihood functions for the increase factor of R_{eff}, modelled based on three studies (solid lines), and resulting posterior probability density (dashed line). The mode is 1.474 and the median is 1.485.

Assuming a multiplicative increase of R_{eff} by the factor 1.48, the infectious dose for aerosol transmission of VOC B.1.1.7 is estimated to be AP_{50} = 1166 (median, 95% CI: 700 – 1942) aerosol particles with diameters between 0.3 and 5 µm.

Literature

1. Endo, A., et al., *Estimating the overdispersion in COVID-19 transmission using outbreak sizes outside China.* Wellcome Open Res, 2020. **5**: p. 67.
2. Hamner, L., et al., *High SARS-CoV-2 Attack Rate Following Exposure at a Choir Practice - Skagit County, Washington, March 2020.* MMWR Morb Mortal Wkly Rep, 2020. **69**(19): p. 606-610.
3. Charlotte, N., *High Rate of SARS-CoV-2 Transmission due to Choir Practice in France at the Beginning of the COVID-19 Pandemic. Available at:*

https://www.medrxiv.org/content/10.1101/2020.07.19.20145326v2. Accessed on: 03 Jan, 2020. , in *medRxiv*. 2020.

4. Miller, S.L., et al., *Transmission of SARS-CoV-2 by inhalation of respiratory aerosol in the Skagit Valley Chorale superspreading event.* Indoor Air, 2020.
5. Hartmann, A., et al., *Emission rate and particle size of bioaerosols during breathing, speaking and coughing. DOI: 10.14279/depositonce-10332. Available at: http://dx.doi.org/10.14279/depositonce-10331; accessed on: 08 Nov 2020.* . 2020.
6. Lednicky, J., et al., *Viable SARS-CoV-2 in the air of a hospital room with COVID-19 patients*, in *medRxiv*. 2020.
7. Dai, H. and B. Zhao, *Association of the infection probability of COVID-19 with ventilation rates in confined spaces.* Build Simul, 2020: p. 1-7.
8. Riley, E.C., G. Murphy, and R.L. Riley, *Airborne spread of measles in a suburban elementary school.* Am J Epidemiol, 1978. **107**(5): p. 421-32.
9. The German Meteorological Service (Deutscher Wetterdienst) https://cdc.dwd.de/portal/202007291339/mapview
10. Wells WF, *Airborne Contagion and Air Hygiene: An Ecological Study of Droplet Infections.* 1955: Cambridge : Harvard University Press (for The Commonwealth Fund), Mass., U.S.A. London : Geoffrey Cumberlege, Oxford University Press.
11. Kriegel, M., et al., *Predicted infection risk for aerosol transmission of SARS-CoV-2; medRxiv. Available at: https://www.medrxiv.org/content/10.1101/2020.10.08.20209106v5. accessed on: 08 Nov, 2020.* . 2020.
12. Backer, J.A., D. Klinkenberg, and J. Wallinga, *Incubation period of 2019 novel coronavirus (2019-nCoV) infections among travellers from Wuhan, China, 20-28 January 2020.* Euro Surveill, 2020. **25**(5).
13. Lauer, S.A., et al., *The Incubation Period of Coronavirus Disease 2019 (COVID-19) From Publicly Reported Confirmed Cases: Estimation and Application.* Ann Intern Med, 2020. **172**(9): p. 577-582.
14. Marks, M., et al., *Transmission of COVID-19 in 282 clusters in Catalonia, Spain: a cohort study.* Lancet Infect Dis, 2021.
15. Buonanno, G., L. Morawska, and L. Stabile, *Quantitative assessment of the risk of airborne transmission of SARS-CoV-2 infection: Prospective and retrospective applications.* Environ Int, 2020. **145**: p. 106112.
16. Fischer, B., C. Knabbe, and T. Vollmer, *SARS-CoV-2 IgG seroprevalence in blood donors located in three different federal states, Germany, March to June 2020.* Euro Surveill, 2020. **25**(28).
17. Edwards, D.A., et al., *Exhaled aerosol increases with COVID-19 infection, age, and obesity.* Proc Natl Acad Sci U S A, 2021. **118**(8).
18. He, X., et al., *Temporal dynamics in viral shedding and transmissibility of COVID-19.* Nature Medicine, 2020. **26**(5): p. 672-675.
19. Reed, L.J. and H. Muench, *A simple method of estimating fifty-percent endpoints.* American Journal of Hygiene, 1938. **27**(3): p. 493 ff.
20. Muller, N., et al., *Severe Acute Respiratory Syndrome Coronavirus 2 Outbreak Related to a Nightclub, Germany, 2020.* Emerg Infect Dis, 2020. **27**(2): p. 645-648.
21. van Doremalen, N., et al., *Aerosol and Surface Stability of SARS-CoV-2 as Compared with SARS-CoV-1.* New England Journal of Medicine, 2020. **382**(16): p. 1564-1567.
22. Efron, B. and T. Hastie, *Computer age statistical inference*. 2016, New York, NY: Cambridge University Press.
23. Sze To, G.N. and C.Y. Chao, *Review and comparison between the Wells-Riley and dose-response approaches to risk assessment of infectious respiratory diseases.* Indoor Air, 2010. **20**(1): p. 2-16.

24. Watanabe, T., et al., *Development of a dose-response model for SARS coronavirus.* Risk analysis : an official publication of the Society for Risk Analysis, 2010. **30**(7): p. 1129-1138.
25. Zellner, A., *Bayesian and Non-Bayesian Analysis of the Log-Normal Distribution and Log-Normal Regression.* Journal of the American Statistical Association, 1971. **66**(334): p. 327-330.
26. Volz, E., et al., *Transmission of SARS-CoV-2 Lineage B.1.1.7 in England: Insights from linking epidemiological and genetic data.* medRxiv, 2021: p. 2020.12.30.20249034.
27. Davies, N.G., et al., *Estimated transmissibility and impact of SARS-CoV-2 lineage B.1.1.7 in England.* Science, 2021. **372**(6538): p. eabg3055.
28. Walker, A.S., et al., *Increased infections, but not viral burden, with a new SARS-CoV-2 variant.* medRxiv, 2021: p. 2021.01.13.21249721.
29. Chowell, G., et al., *Mathematical and statistical estimation approaches in epidemiology*. Mathematical and Statistical Estimation Approaches in Epidemiology. 2009: Springer, Dordrecht.
30. Graham, M.S., et al., *Changes in symptomatology, reinfection, and transmissibility associated with the SARS-CoV-2 variant B.1.1.7: an ecological study.* Lancet Public Health, 2021.

Supplement table 1: Symptom frequency among cases of choir 1 (N=58).

Symptom	n with information	n with symptom	Proportion among those with information	Proportion among all
			%	%
Fatigue	54	46	85	79
Cephalgia	56	39	70	67
Cough	53	33	62	57
Loss of taste (partial)	51	18	35	31
(complete)		14	27	24
Loss of smell (partial)	52	13	25	22
(complete)		18	35	31
Body pain	54	30	56	52
Sore throat	51	27	53	47
Fever	50	26	52	45
Chills	52	22	42	38
Rhinorrhoea	52	22	42	38
Dyspnea	50	18	36	31
Nasal congestion	44	13	30	22
Diarrhoea	48	13	27	22
Nausea	51	9	18	16
Exanthema	49	5	10	8.6
Pneumonia	41	2	4.9	3.4

Supplement table 2: Mutations and amino acid substitutions in all sequenced genomes, i.e. the outbreak strain EPI_ISL_753922 and the "outlier" strain EPI_ISL_753799. Reference strain is Wuhan-HU-1.

		Mutation (position) Aminoacid substitution										
		241	**3037**	**10525**	**14408 ORF1b: P314L**	**19065**	**21137 ORF1b: K2557R**	**22303 S:S247R**	**23403 S:D614G**	**24198 S:A879V**	**26144 ORF3a: G251V**	**29751-29760 9 bp gap**
Origin	Isolate											
	Wuhan-HU-1	C	C	C	C	T	A	T	A	C	G	-
Choir 1	EPI_ISL_753799	C	C	C	C	C	A	G	A	C	T	+
Choir 1	EPI_ISL_753922	T	T	C	T	T	G	T	G	C	G	-
Choir 1	EPI_ISL_1804962	T	T	C	N	T	G	T	G	C	G	-
Choir 1	EPI_ISL_753921	T	T	C	T	T	G	T	G	C	G	-
Party	hCoV-19/Germany/RKI-Z-0046/2020	T	T	C	T	T	G	T	G	C	G	-
Party	hCoV-19/Germany/RKI-Z-0047/2020	T	T	C	T	T	G	T	G	C	G	-
Party	hCoV-19/Germany/RKI-Z-0048/2020	T	T	C	T	T	G	T	G	C	G	-
Choir 1	hCoV-19/Germany/RKI-Z-0049/2020	T	T	C	T	T	G	T	G	C	G	-
Choir 1	hCoV-19/Germany/RKI-Z-0050/2020	T	T	T	T	T	G	T	G	C	G	-
Choir 1	hCoV-19/Germany/RKI-Z-0051/2020	T	T	C	T	T	G	T	G	C	G	-
Choir 1	hCoV-19/Germany/RKI-Z-0052/2020	T	T	C	T	T	G	T	G	T	G	-
Choir 1	hCoV-19/Germany/RKI-Z-0053/2020	T	T	C	T	T	G	T	G	C	G	-
Choir 2	hCoV-19/Germany/RKI-Z-0054/2020	T	T	C	T	T	G	T	G	C	G	-
Choir 1/2	hCoV-19/Germany/RKI-Z-0055/2020	N	T	C	T	T	G	T	G	C	G	-

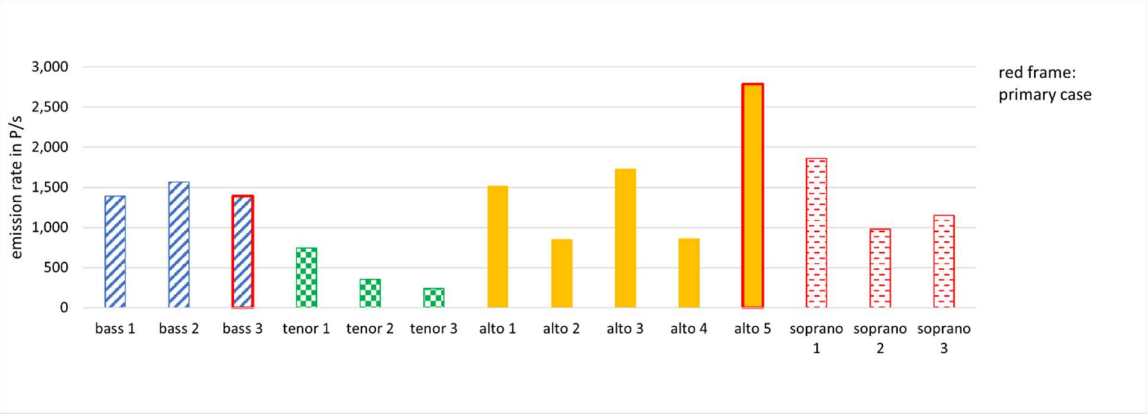

Supplement figure 1: cumulative emission while singing "Liverpool Oratorio"

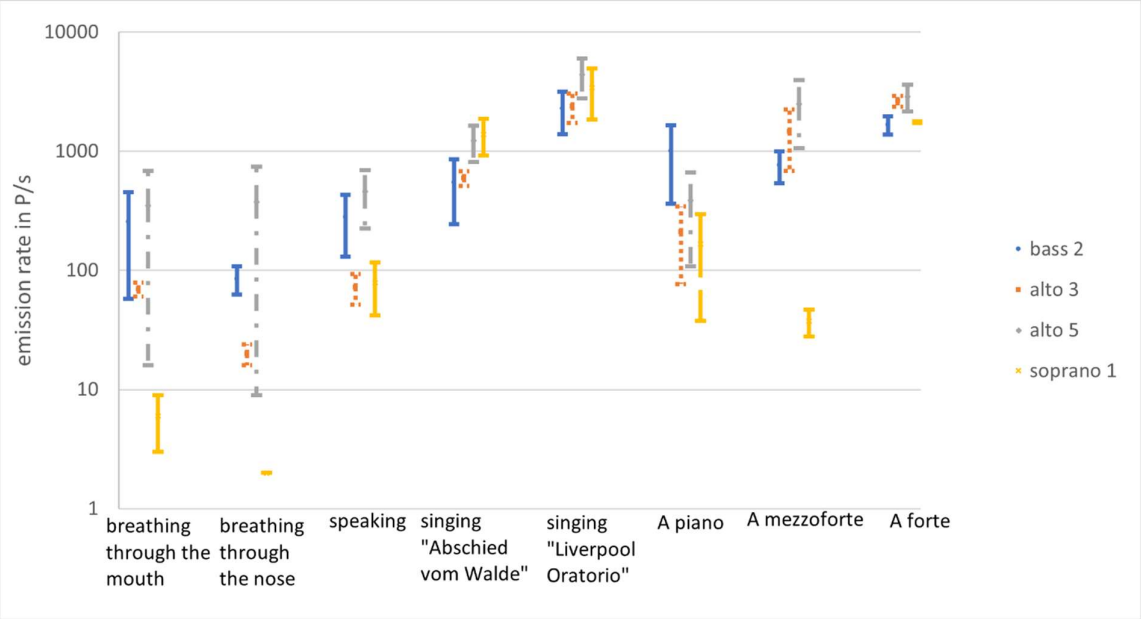

Supplement figure 2: comparison of the emission rates for the subjects, whose measurements were repeated at different days